Published in final edited form as:
Clin Cancer Res. 2008 November 15; 14(22): 7367–7377. doi:10.1158/1078-0432.CCR-08-1016.

Diabodies targeting epithelial membrane protein 2 reduce tumorigenicity of human endometrial cancer cell lines

Kaori Shimazaki[1], **Eric J. Lepin**[2], **Bo Wei**[3], **Agnes K. Nagy**[3], **Catherine P. Coulam**[3], **Sergey Mareninov**[3], **Maoyong Fu**[3], **Anna M. Wu**[2], **James D. Marks**[4], **Jonathan Braun**[1,2,3], **Lynn K. Gordon**[5,*], and **Madhuri Wadehra**[3,*]

[1] Molecular Biology Institute, University of California, Los Angeles, California 90095

[2] Crump Institute for Molecular Imaging, Department of Molecular and Medical Pharmacology, David Geffen School of Medicine at UCLA, Los Angeles, California 90095

[3] Department of Pathology and Laboratory, David Geffen School of Medicine at UCLA, Los Angeles, California 90095

[4] Anesthesia and Pharmaceutical Chemistry at UCSF, San Francisco, California, 94143

[5] Jules Stein Eye Institute, University of California, Los Angeles, California 90095, and Department of Surgery, Greater Los Angeles Veterans Affairs Healthcare System, Los Angeles, California 90099

Abstract

Purpose—Endometrial cancer (EC) is the most common gynecologic malignancy. One promising biomarker is epithelial membrane protein-2 (EMP2), and its expression is an independent prognostic indicator for tumors with poor clinical outcome expression. The present study assesses the suitability of EMP2 as a therapeutic target.

Experimental Design—Human monovalent anti-EMP2 antibody fragments were isolated from a human phage display library, and engineered as bivalent antibody fragments (diabodies) with specificity and avidity to both EMP2 peptides and native cell-surface EMP2 protein. Diabodies were assessed using cell death and apoptosis assays. In addition, the efficacy of EMP2 diabodies on EC tumors was determined using mouse xenograft models.

Results—Treatment of human endometrial adenocarcinoma cell lines with anti-EMP2 diabodies induced significant cell death and caspase 3 cleavage in vitro. These responses correlated with cellular EMP2 expression, and were augmented by progesterone (which physiologically induces EMP2 expression). *In vivo*, treatment of subcutaneous human xenografts of HEC-1A cell lines with anti-EMP2 diabodies suppressed tumor growth, and induced striking xenograft cell death.

Conclusions—These findings suggest that EMP2 may be a potential pharmacological target for human EC.

Keywords

Epithelial membrane protein 2; endometrial cancer; phage display; antibody therapy

[*]To whom correspondence should be addressed: Madhuri Wadehra, Pathology and Lab Medicine, 14-127 Center for Health Sciences, Geffen School of Medicine at UCLA, Tel: 310-825-1590, Fax: 310-825-5674, mwadehra@mednet.ucla.edu. Lynn Gordon, Jules Stein Eye Institute, 100 Stein Plaza, Geffen School of Medicine at UCLA, Tel: 310-206-4803, Fax: 310-796-7906, lgordon@ucla.edu.

Introduction

Endometrial cancer (EC) is the most common gynecological malignancy. In the United States, more than 41,000 new cases and 7,300 deaths were estimated in 2006 (1). EC is classified into two major sub-groups based on histology, clinical behavior, and epidemiology. The more common Type I is associated with estrogen predominance and pre-malignant endometrial hyperplasia (2, 3). Type II is mediated by non-hormonal risk factors, and often has a high grade or high-risk histology with an aggressive clinical course (2). Incidence of ECs generally increases with age, and 75–80% of new cases are found in postmenopausal women (4).

Primary treatment for ECs is the surgical removal of the tumor, but recurrence is common, and other therapeutic interventions (radiotherapy, chemotherapy, and endocrine therapy) benefit only a subset of patients (5, 6). Presently, there are few biomarkers that distinguish ECs at the pre-malignant stage, although emerging efforts are targeting molecules that underlie the process of tumorigenesis (7, 8). Similarly, there are currently no biomarkers that can be targeted for tumor suppression and elimination. Thus, new modalities for early detection and treatment of ECs at premalignant and frankly malignant stages of disease are needed to improve management and prognosis.

One promising biomarker appears to be epithelial membrane protein-2 (EMP2). EMP2 expression is associated with EMP2 neoplasia (21). In endometrial cancer, EMP2 is an independent prognostic indicator for tumors with poor clinical outcome. EMP2 positive tumors, compared to EMP2 negative tumors, had a significantly greater myometrial invasiveness, higher clinical state, recurrent or persistent disease following surgical excision, and earlier mortality. As EMP2 expression was independent of other known biomarkers such as the estrogen receptor and progesterone receptor (21), EMP2 represents a unique biomarker for patients who are not responsive to current hormone or chemotherapy. Moreover, EMP2 expression level positively correlates with the increasing pre-malignant potential of proliferative endometrium. That is, there is a gradation of endometrial EMP2 expression, with minimal expression in normal proliferative or quiescent premenopausal endometrium, and increasing expression in patients with disordered proliferative endometrium, endometrial hyperplasia, and endometrium carcinomas.

EMP2 is a member of the growth arrest specific gene 3/peripheral myelin protein 22 (GAS3/PMP22) four transmembrane protein family with distinctive biochemical and physiological roles (9–11). In the endometrium, EMP2 expression is regulated by progesterone and required for successful blastocyst implantation (19–21). EMP2 appears to regulate trafficking of various proteins and glycolipids by facilitating transfer of molecules from post-Golgi endosomal compartments to appropriate plasma membrane locations. Specifically, EMP2 is thought to facilitate the appropriate trafficking of select molecules into glycolipids-enriched lipid raft microdomains (GEMs) (10). GEMs are cholesterol rich microdomains which are often associated with chaperones, receptosomes, and protein complexes that are important for efficient signal transduction (12, 13). Moreover, GEMs are involved in correct sorting of proteins from the Golgi apparatus to plasma membrane (14–16). In this respect, modulation of EMP2 expression levels or its location on the plasma membrane alters the surface repertoire of several classes of molecules including integrins, focal adhesion kinase, class I major histocompatibility molecules and other immunoglobulin super-family members such as CD54 and GPI-linked proteins (10, 11, 17, 18)

The basic receptor cell biology of EMP2 (controlling surface display and signaling function) and its prognostic association with EC and premalignant states suggested that EMP2 may be a pharmacologic target in EC. In this study, we tested this idea by selecting human anti-

EMP2 diabodies from single chain Fv (ScFv) antibody library (22), and engineering them as small bivalent antibody fragments (diabodies), which have unique practical applications because of their avidity, specificity, and small size (23). Recently, diabodies were found to undergo rapid tumor uptake and fast blood clearance in murine models, showing their potential for immunodiagnosis and therapies for cancer (24). Here, we show that in vitro treatment of endometrial adenocarcinoma cells with anti-EMP2 diabodies dramatically decreased cell proliferation by upregulating caspase-dependent apoptosis. Moreover, anti-EMP2 diabodies were effective in reducing tumor size and inducing cell death in human EC xenografts. These data suggest that pharmacological manipulation of EMP2 may be a candidate target for EC therapy.

Methods

Cell lines

The human endometrial adenocarcinoma cell line HEC-1A (HTB112, ATCC, Manassas, VA), RL95-2 (CRL 1671, ATCC), Ishikawa (gift of Dr. Mark Pegram, UCLA), and mouse embryonic fibroblast cell line NIH 3T3 (CRL-1658, ATCC) were cultured in appropriate media supplemented with 10% fetal calf serum at 37°C in a humidified 5% CO_2 and passaged every 7 days. In addition to HEC-1A wild type cells (HEC-1A/WT), HEC-1A sublines were prepared to increase or decrease EMP2 expression using expression plasmids for a human EMP2-GFP fusion protein and control GFP (20). These sublines were termed HEC-1A/OE, HEC-1A/V, respectively. EMP2 expression levels in each cell line were determined by Western blot analysis.

Phage library selection

Phage library selection was carried out as previously described (25). Briefly, 10^{12}–10^{13} phage from the 8.2×10^8 member phagemid library were first pre-depleted with 100μL of streptavidin magnetic beads (Invitrogen, Carlsbad, CA) in 2% milk PBS for 1 hour at room temperature. The pre-depleted phage library was then mixed with 10 μg of biotin conjugated 24 amino acid peptides corresponding to the extracellular loop of human and mouse EMP2 (DIHDKNAKFYPVTREGSYGGSGSK and DLHQQNRKLYYLLQEGSYGGSGSK respectively) (26) for 1 hour at room temperature. 100 μL of 2% milk PBS pre-blocked streptavidin magnetic beads were added to the phage mixture and rotated for 15 min at room temperature. Beads were washed extensively with 0.1% PBS/Tween, 2% milk PBS, and finally with PBS, and bound phage was eluted out with 1mL of 100mM triethylamine, neutralized with 500 ul of 1M Tris-HCl pH 7.4, and added to 10 mL of exponentially growing *E. coli* TG1. Culture was then plated on 150mm culture plates with 2x TY 100μg/ml ampicillin, 2% glucose agar plates (2X TY/amp/glu) overnight at 37°C. The next day, colonies were scraped from the plates and used to amplify the phage for the second round of selection described above. A total of three selections were performed before screening and characterization of the selected phage antibodies.

Diabody construction and production

Binding specificity of expressed single chain Fv (ScFv) was analyzed by Enzyme-Linked ImmunoSorbent Assay (ELISA) as previously described (22) (see ELISA section below for details). Single chain Fv clones with high reactivity were selected for the construction of diabodies. A number of different ScFv clones were characterized and confirmed by DNA fingerprinting (27, 28) and DNA sequencing (29). pHEN phagemids from selected phage were isolated using QIAprep Spin Miniprep Kit (Qiagen, Valencia, CA). Single chain Fv inserts were then digested and cloned into pSYN I vector in frame with a c-Myc and 6 His tag at the C-terminus. In order to convert ScFv fragments into diabody, 15 amino acid linker region (AGTGGTGGAGGCGGTTCAGGCGGAGGTGGCTCTGGCGGTGGCGGATCG)

of the ScFv was shortened into 5 amino acid linker (AGTGGTGGAGGATCG) using QuikChange site-directed mutagenesis kit (Stratagene, La Jolla, CA) (30). Deletion mutation was confirmed by DNA sequencing analysis.

Expression and purification of the selected diabodies were carried out using a modified protocol described by Marks et al. (22). Single colonies were picked from the plate, inoculated into 1L/colony of 2 X TY with 100 μg/mL ampicillin (2X TY/amp) at 250 rpm at 37°C. When A_{600} reached 0.8 – 1.0, protein expression was induced by addition of 1 mM IPTG. The culture was shaken at 120 rpm at 30°C for 4 hours and spun at 7000 rpm for 15 min at 4°C. Pellets were then re-suspended in 20 mL of periplasmic buffer (200mM Tris-HCl, 20% sucrose, 1 mM EDTA, pH 7.5), and 290,000 units of lysozyme (Epicentre, Madison, WI) was added to each mixture. The mixtures were incubated at room temperature for 5 min and spun at 7000 rpm for 15 min at 4°C. The pellets were then re-suspended with 20ml of 40mM $MgSO_4$ and left on the ice for 10 min. The samples were spun again, and the supernatants from this spin were combined with the first supernatants. The mixture was then filtered with 0.45μm filters, and dialyzed in dialysis buffer (300mM NaCl, 20mM HEPES, pH 8.0) overnight at 4°C. Next morning, the samples were filtered again with 0.2 μm filters and run through 5 mL of the Ni-NTA column (Qiagen). The column was washed with 20 mL wash buffer (300 mM NaCl, 20 mM imidazole, 20 mM HEPES, 0.05% Tween, pH 8.0), and bound diabodies were eluted with 5ml elusion buffer (300 mM NaCl, 250 mM imidazole, 20 mM HEPES, pH 8.0), dialyzed in endotoxin free PBS overnight at room temperature. Samples were filtered with 0.22 μm filters, and stored at −20°C until their use. Purity of the preparation was determined by size exclusion chromatrography profile (FPLC; Superdex 75, Amersham Pharmacia Biotech, Uppsala, Sweden) as necessary.

For preparative analysis of the diabody, purified diabody preparations were run on 4–20% Tris-Glycine gel (Invitrogen) and bands were visualized using GelCode Blue Stain Reagent (Pierce, Rockford, IL). Gels were scanned and the band intensities were analyzed using the Image J program (National Institute of Health, Bethesda, MD).

Enzyme-linked immunosorbent assay (ELISA)

10 μg/mL of biotinylated 24 amino acid peptides (see the phage library selection section above) were coated onto streptavidin-coated 96-well plates (Roche Applied Science, Indianapolis, IN) in PBS for 1 hour at room temperature. Plates were then washed with PBS and blocked with 2% milk PBS for 2 hours at 37°C. Expressed phage antibodies or diabodies were added to each well, incubated at room temperature for 1 hour, and washed with 0.05% PBS/Tween three times. Bound antibodies or diabodies were detected with mouse anti-c-Myc (9E10) antibody (Calbiochem, San Diego, CA), followed by horseradish peroxidase (HRP) conjugated anti-mouse antibody (BD Bioscience Pharmingen, Franklin Lakes, NJ) and TMB solution (eBioscience, San Diego, CA). Plates were read by microplate reader Model 550 (Bio-Rad, Hercules, CA) at 450nm.

Fluorescent activated cell sorting (FACS) analysis

Cells were detached from a flask with 2mM EDTA, spun at 1000 rpm for 3 min, and re-suspended with BD Cytofix/Cytoperm solution (BD Bioscience Pharmingen) to final concentration of 1×10^7 cells/mL. Cells were washed with BD Perm/Wash buffer (BD Bioscience Pharmingen), followed by a 30min incubation with BD Perm/Wash buffer containing 2% BSA on ice. After spinning at 2000rpm, cells were resuspended with BD Perm/Wash buffer containing 1 μg of purified monoclonal diabody in 96 well plates on ice for 1 hour. Cells were then washed with 200 μL of BD Perm/Wash buffer three times. Bound monoclonal diabodies were detected with mouse anti-c-Myc (9E10) antibody

(Calbiochem), followed by R-PE conjugated anti-mouse secondary antibody (BD Bioscience Pharmingen).

Serum stability assay

Diabody preparations were diluted in 200 μL of human or mouse serum to a final concentration of 5 μg/mL and plated in a 96 well plate. The plate was incubated at 37°C for 15 min, 24 hours, 48 hours, or 72 hours. Samples were collected, and the diabody serum stability was determined via ELISA method described above.

Cellular Cytostasis

5×10^4 cells were incubated in 96 well plates with 0–25 μg/mL diabody. At 0 and 24 hours, cells were stained with toluidine blue, and then lysed in 2% SDS (Biowhittaker, Walkersville, MD). The number of cells at each timepoint was quantitated in triplicate by the absorbance at 595 nm, and the standard error of the mean was calculated. Each experiment was repeated at least three times.

Cell death analysis

For cell death analysis, cells (5×10^5) were incubated in 6-well plates in 10% FCS medium. Cells were incubated with 12.5 μg/ml diabody A10 (control), KS49, or KS83 for 72 hrs. For hormone treatment, RL95-2 cells at 60–70% confluence were washed in PBS, and subsequently incubated with progesterone (Sigma., St. Louis, MO) in treatment medium (DMEM/Ham's F-12 supplemented with 0.5% charcoal-stripped FBS (Omega Scientific, Tarzana, CA), 1% penicillin-streptomycin, and 1% L-glutamine). Progesterone was and added to treatment medium at 25 μM as previous described (31). Cell viability was determined by trypan blue exclusion.

To determine the rate of apoptosis, cells were stained with annexin V (Becton Dickinson Biosciences, Torrey Pines, CA) and 7-aminoactinomycin D (7AAD) or propidium iodide. Cells were harvested at 24–48 hours after diabody treatment as indicated in the figure legends. The cells were incubated for 15 minutes on ice with annexin V-Cy3 and 7AAD as per manufacturer's instructions, and analyzed on a flow cytometer (Becton Dickinson Biosciences).

Caspase 3 activity

Cells were incubated as above and harvested 48 hours after diabody treatment. Samples were normalized based on cell number and lysed by boiling for 5 minutes in Laemmli buffer (62.5 mM Tris-Cl, pH 6.8, 10% glycerol, 2% SDS, 0.01% bromophenol blue, 2% βME). The lysate was separated on a 12% SDS-polyacrylamide gel and transferred to a nitrocellulose membrane (Amersham Pharmacia). Membranes were incubated with 10% milk in PBS containing 0.1% Tween-20. An anti-caspase 3 mouse monoclonal antibody, 2 ng/μL final concentration (BD Biosciences), or anti-β-actin (Sigma) was added and incubated for 1 hour. The membrane was washed 3 times with PBS/Tween-20 and then incubated for 45 minutes with a horseradish peroxidase-labeled secondary antibody (goat anti-mouse immunoglobulin G [IgG] or goat anti-rabbit IgG, 1:2000 dilution; Jackson ImmunoResearch Laboratories, West Grove, PA). Proteins were detected by chemiluminescence (Amersham Pharmacia).

Native tissue toxicity

Six to eight week old female wildtype (C57BL/6) mice were obtained from JAX laboratories. Animals were inoculated intravenously with increasing concentrations (0.5–5 mg/kg) of A10 diabody control, anti-EMP2 diabodies (K83, K49), or a vehicle control

(sterile PBS). Three mice were utilized per group and were injected twice a week. After 14 days, serum was collected, and mice were euthanized by cervical dislocalization. Tissue (kidney, liver, spleen, lung, skin) were collected and fixed in formalin. Samples were processed by the Tissue Procurement Laboratory at UCLA. Toxicity in tissue was assessed using hemotoxylin and eosin and validated by a pathologist. Serum alanine aminotransferase (ALT) and direct and total bilirubin were assessed by the UCLA Medical Center Clinical Laboratories.

Tumor xenografts and treatment

Four to six-week-old nude BALB/c female mice were obtained from Charles River Laboratories (Wilmington, MA) and maintained at the University of California, Los Angeles in accordance with IRB procedures. Animals were inoculated s.c. with 1×10^6 HEC-1A/V and HEC-1A/OE cells into the right and left shoulder flanks. Once tumors reached 2–3mm (largest diameter, day 13), tumors were injected biweekly with 1 mg/kg anti-EMP2 diabody 83, control diabody 10, or a vehicle control (sterile saline) for up to three weeks. Six mice were utilized per group. Tumors were measured every 3–4 days using vernier calipers, and tumor volumes were calculated by the formula $\pi/6 \times$ larger diameter $\times$ smaller diameter (32). At day 30, tumors were excised and fixed in formalin. Tumors were processed for hemotoxylin and eosin staining by the Tissue Procurement Laboratory at UCLA.

Statistical analysis

For the ELISA analysis, groups were analyzed by two-tailed Student's paired t-test at a 95% confidence level. Differences in the *in vitro* anti-proliferative and in vivo effects of diabodies were evaluated using Student's unpaired t-test at a 95% confidence level (GraphPad Prism version 3.0; GraphPad Software, San Diego, CA).

Results

Construction and expression of anti-EMP2 diabodies

Anti-EMP2 scFv was isolated using phage library expressing 8.2×10^8 variable scFv as previously described (25). EMP2 specific scFv were selected using 24 amino acid-long peptides that represent second extracellular domain (ECD) of human (hEMP2) and mouse EMP2 (mEMP2). Fourteen clones were identified by hEMP2 ELISA, and of these, three independent clones were found to be independent by sequence features. Three independent clones were constructed and produced as diabodies; all were positive by ELISA, and one (KS49) was positive by flow cytometry for native EMP2 binding (see below). Fourteen clones were identified by mEMP2 ELISA, and of these, three independent clones were found to be independent by sequence features. Three independent clones were constructed and produced as diabodies; all were positive by ELISA, and one (KS83) was positive by flow cytometry for native EMP2 binding. As negative controls, two random pre-selection scFvs were chosen (A10 and B3): none were positive by ELISA with hEMP2 or mEMP2 in either the scFv or diabody format.

For the present study, KS49 and KS83 were chosen as representative scFv for hEMP2 and mEMP2, respectively. Two random pre-selection scFv, A10 and B3, were used as negative control antibodies. In order to increase the avidity of the selected scFv, we created divalent diabodies by shortening the scFv linker region to 5 amino acids (Fig 1A) (30). Diabodies were expressed in TG1 *E. coli* and purified as previously published (see Methods).

SDS-PAGE and size exclusion FPLC analysis of purified anti-EMP2 diabodies

Analysis of purified diabody proteins by SDS-PAGE in a reducing condition showed a single band around 25kDa, which corresponds to an appropriate size of scFv or diabody

monomer (Fig. 1A) (24). Size exclusion chromatography also demonstrated the formation of a dimer with a protein retention time at 20.23 min (average of two experiments), matching with the expected size of the diabody (Fig. 1B) (24). Both data indicated >95% purity of the prepared diabody samples.

Antigen specificity of anti-EMP2 diabodies

Specificity and titer of selected diabodies were initially tested by ELISA using plates coated with hEMP2 or mEMP2 peptides. KS49, a diabody selected against hEMP2 peptide, showed significant binding to hEMP2, whereas binding to mEMP2 was below detection (data not shown). Reciprocally, KS83, a diabody selected against mEMP2 peptide, showed high reactivity to mEMP2 peptide, whereas reactivity to hEMP2 peptide was below detection (data not shown). Negative control diabodies A10 and B3 demonstrated minimal reactivity to either hEMP2 or mEMP2 peptides. As shown in Fig. 1C and D, diabody titration analysis showed a dose-dependent binding of the KS49 and KS83 to the hEMP2 and mEMP2 antigens respectively. KS49 and KS83 efficiently bound to their appropriate antigen with EC_{50} (the antibody concentration at which 50% of maximum binding occurs) of 53.1ng/mL and 9.32ng/mL, respectively. Using monovalent scFv products of these two antibodies, the EC_{50} for cognate EMP2 peptide was >2 μg/mL (data not shown). Thus, divalency contributed to the avidity of the two anti-EMP2 diabodies.

Binding activity of diabodies was further assessed by FACS analysis using human endometrial adenocarcinoma cell lines RL95-2, Ishikawa, and the murine fibroblast cell line NIH 3T3, all of which are known to express EMP2 (representative data shown in Fig. 2). Both KS49 and KS83 showed significant reactivity against all three cell lines regardless of the difference in host species. This species cross reactivity may reflect the close homology between human and mouse EMP2 second extracellular domains (50% sequence identity and 90% sequence similarity; see Methods). Control diabodies A10 and B3 showed minimal detection against all cell lines, confirming the specificity of the anti-EMP2 diabodies against EMP2 proteins.

Diabody stability in serum

One of the practical usages of diabodies is therapeutic targeting of cancer tumors (33). In order to assess the stability of anti-EMP2 diabodies in physiological condition, 5μg/mL of diabodies were incubated in either human or mouse serum at 37°C for 15min, 24, 48, and 72 hours. The retained stability was measured using an ELISA. The binding activity of the diabody was maintained over the 72 hour-period in both human and mouse serum (data not shown). The specificity, which was detected using relevant and irrelevant peptide antigens, was also retained for the prolonged incubation period.

Antibodies to EMP2 inhibit cellular growth

To determine if selective targeting of EMP2 may be an effective therapy in EC, the endometrial adenocarcinoma cell lines RL95-2, Ishikawa, and HEC-1A-WT were utilized. Cells were treated with KS49, KS83, or the control diabody A10 (Fig. 3). Compared to control diabody, anti-EMP2 diabodies induced cellular cytostasis within 24 hours. When cells were incubated with a range of recombinant antibody from 0–25 μg/mL, the recombinant clones KS49 and KS83 had a dose-dependent, anti-proliferative effect on the endometrial cell lines RL95-2 and Ishikawa (Fig. 3A and C). In contrast, diabodies against EMP2 exhibited small effects on HEC-1A-WT cells, which have been shown to bear little EMP2 on the plasma membrane (19, 20). However, upon up-expression of EMP2 in these cells, diabody KS83 and KS49 significantly inhibited growth of HEC-1A/OE cells by 55% and 21%, respectively (Fig. 3B and D).

Diabodies to EMP2 induce apoptosis

To correlate the decrease in cell number with an increase in cell death, cells were assessed for apoptotic cells using flow cytometry. Endometrial carcinoma cell lines were treated with 12.5 μg/mL KS49, KS83, or control A10 diabodies for 24 hours. Apoptotic cells were detected with annexin V and 7-AAD and analyzed by flow cytometry. Anti-EMP2 diabodies induced pronounced cell death in RL95-2 cells (Fig. 4A). Small effects were seen in HEC-1A-GFP cell lines, but cell death was enhanced by overexpression of EMP2 (HEC-1A/OE) (Fig. 4B and C). Thus, anti-EMP2 diabodies specifically increased apoptosis, in a manner associated with increased EMP2 surface expression.

Synergistic effects of progesterone

Previous studies have suggested that EMP2 expression is regulated by progesterone (31). As progesterone increases EMP2 expression, we predicted that progesterone treatment may enhance the rate of anti-EMP2 diabody mediated apoptosis in RL95-2 cells as these cells express functional progesterone receptors (34, 35). Cells were stained with annexin V and propidium iodide and analyzed by flow cytometry. Dramatically, the combination of progesterone (P4) and KS49 or KS83 treatment increased the number of annexin V, propidium iodide positive cells by 16.5% and 19% respectively compared to cells treated with diabody alone (Fig. 5A).

To confirm that combination progesterone and EMP2 specific diabodies increase cell death over diabody treatment alone, cells were analyzed by trypan blue exclusion 72 hours after treatment (Fig. 6B). Progesterone and KS83 or KS49 significantly increased cell death over progesterone and control diabody A10 treatment ($p<0.01$ and $p<0.04$; Fig. 6B). Moreover, progesterone significantly increased KS83 diabody treatment by 19.1 ± 3% over KS83 treatment alone ($p<0.05$). Although not significant, progesterone also increased KS49 mediated cell death by 8.1 ± 3% over KS49 treatment alone ($p=0.07$).

The annexin V and propidium iodide staining suggested that anti-EMP2 diabodies induced an apoptotic mode of cell death in RL95-2 cells. To validate this effect, cells were treated with 12.5 μg/ml of the EMP2 specific diabodies KS83 and KS49 or control diabody A10 in the presence or absence of progesterone for 24–36 hours. Active caspase 3 was measured in equivalent cell lysates by western blot analysis (Fig. 5C and D). As expected, significant differences in cleaved caspase 3 was detected upon addition of KS83 compared to the control diabody A10 ($p<0.05$). Strikingly, significantly higher levels of activated caspase 3 were detected upon addition of progesterone and KS49 and KS83 compared to the control A10 ($p<0.05$; $p<0.01$, respectively). These results suggest that progesterone and KS49 or KS83 act synergistically to induce apoptosis of endometrial cancer cells.

In vivo tumor targeting

In order to evaluate the preclinical efficacy of EMP2 therapy, the toxicity of two anti-EMP2 diabodies (KS49 and KS83), and a control diabody (A10) were assessed for toxicity in wildtype C57BL/6 mice. KS49 and KS83 bind a shared epitope in mouse and human EMP2, and are thus useful for assays for toxicity to normal tissues, as well as therapeutic modeling in xenograft assays. To assess normal tissue toxicity, anti-EMP2 and control diabodies were parenterally administered each two days (ranging up to 9 mg/kg) over two weeks in wildtype mice (C57BL/6). No changes were observed in animal weight, or in serum metabolic analytes for liver function (Table 1). Gross and microscopic examination of tissues also showed no abnormalities (data not shown). Notably, this examination reflected an absence of toxicity in lung and skin, which express high levels of EMP2. Thus, in this limited analysis, no toxicity was detectable by anti-EMP2 diabody to normal tissues.

In order to evaluate the efficacy of anti-EMP2 diabodies in vivo, an endometrial cancer xenograft model was created. Tumors from HEC-1A/V and HEC-1A/OE cells were established in the shoulder flanks of female BALB/c nude mice. After detectable tumor formation (day 13), anti-EMP2 KS83, control A10, or a vehicle control (sterile saline) were injected biweekly intra-tumorally, and progression of tumor size was measured by calipers. By day 30, KS83 had profoundly inhibited tumor growth of both HEC-1A/V and HEC-1A/OE tumors (Figure 6).

Excised tumors at day 30 revealed greater than 4-fold differences in tumor size between KS83 and A10 treatment in HEC-1A/V cells (Fig. 6C, D) and HEC-1A/OE cells (data not shown). In addition, hemotoxylin and eosin staining revealed large areas of necrosis in tumors treated with KS83 but not with A10 or the vehicle control in HEC-1A/V tumors (Fig. 6C). Necrosis was more pronounced in KS83 treated HEC-1A/V than HEC-1A/OE tumors, perhaps the result of clearance by immune cells (Fig. 6D).

Discussion

In this study, we developed recombinant human anti-EMP2 diabodies using filamentous bacteriophage library methodology, and assessed the efficacy of these diabodies in growth, apoptosis, and xenograft tumor formation by EC cell lines. Diabody avidity and specificity for EMP2 peptide and native protein were confirmed by ELISA and flow cytometry using multiple cell lines. Biologically, treatment of various human endometrial adenocarcinoma cell lines with these anti-EMP2 diabodies resulted in a significant increase in caspase-dependent apoptotic cell death in vitro, and reduced tumor volume and viability in vivo. These data suggest that EMP2 is a targetable molecule for pharmacological induction of apoptosis in EC cell lines.

It was notable that a human immunoglobulin gene library permitted successful production of anti-human EMP2 antibodies. While these antibodies in effect detected a self-antigen, they should not be construed as a native autoimmune specificity, since the combinatorial library permits the creation of VH/VL pairings that may not have been represented in the native clonal populations (22). Conversely, the direct yield of human immunoglobulin reagents with such biologic activity avoids the complexity of reengineering non-human epitopes while retaining antigen specificity and avidity in rodent-derived reagents (36).

Successful therapeutic targeting of antibodies depends on tissue penetration and uptake, rapid blood clearance, and serum stability. Small antibody fragments such as scFv have rapid tissue penetration and fast clearance from the circulation, but as monovalent reagents are limited by low binding affinity and avidity (37–40). Accordingly, we engineered selected anti-EMP2 scFv fragments into bivalent diabodies, which are known to have an increased avidity and stability, by shortening the linker region of scFv's between heavy chain variable region (V_H) and light chain variable region (V_L) (41, 42), SDS-PAGE and size exclusion FPLC data confirmed successful diabody formation with >95% purity, and >20-fold increase in binding activity compared to original scFvs.

FACS analysis of anti-hEMP2 and anti-mEMP2 diabodies demonstrated significantly elevated reactivity against surface EMP2 compared to controls. Interestingly, both anti-hEMP2 and anti-mEMP2 diabodies showed cross-species reactivity against human and mouse EMP2. It should be noted that the selecting hEMP2 and mEMP2 peptide antigens shared 90% sequence similarity and 50% sequence identity. Thus, it appeared that the key contact residues for this set of anti-EMP2 diabody clones were included among these species-conserved homologous peptides. Since the cross-species epitope was not detected with the free peptide, we surmise that the native protein constrained the topology of the

epitope to increase avidity of diabody binding. The strong cross-species homology of the EC2 peptide, and this apparent topological display suggest that this epitope may be biologically important for the native function of EMP2.

Anti-EMP2 diabody treatment exhibited significant anti-proliferative effects by increasing caspase 3-related apoptosis in multiple endometrial adenocarcinoma cell lines. These effects on cell growth inhibition and apoptosis correlated with EMP2 expression levels of independent cell lines, suggesting that binding of EMP2 induced apoptosis signaling. In support of this idea, progesterone induction of EMP2 expression increased diabody-mediated cell death in RL95-2 cells. Alternatively, recent data has shown that intravaginal injection of anti-EMP2 diabody in the murine genital tract dramatically reduced EMP2 expression in native endometrial epithelium (43). It should be noted that EMP2 exists in a physical complex with FAK and certain integrin isoforms and promotes FAK-Src activation (18). Since divergent signaling pathways are induced by integrin ligation, it is conceivable that apoptosis may be favored in the absence of FAK (44–46).

In order to determine the preclinical applicability of targeting EMP2, toxicity experiments were initially performed. Importantly, anti-EMP2 diabody treatment exhibited minimal toxicity as measured by weight loss, liver function, and changes in histology when administered systemically over a two week time frame. Furthermore, the reduction in tumor volume for both HEC-1A/V and HEC-1A/OE cells with anti-EMP2 diabodies suggest that targeting EMP2 may be a successful for treatment. Interestingly, HEC-1A/V cells, which express modest levels of EMP2 on the plasma membrane in culture, responded significantly to anti-EMP2 diabody treatment. We predict that this may be the result of prolonged treatment (18 days), or the result of extrinsic factors (such as steroid hormones) which may increase EMP2 expression. Additional experiments will need to be performed to evaluate the changes in EMP2 expression and changes induced by anti-EMP2 diabodies in vivo.

Apoptosis can involve activation of diverse caspase isoforms, depending on the death receptor-mediated and mitochondrial pathways of apoptosis induction (47). In this study, caspase 3 activation was assessed, since it is the downstream event of all of these pathways (47). We note that EMP2 is important for integrin expression and function, and also modifies surface display of GEMs and their associated membrane proteins (see Introduction). Accordingly, EMP2 may modulate integrin-dependent signaling associated with survival signaling, or by other GEM-associated receptors. For example, K-ras and HER-2/*neu* has been identified as an EC-associated oncogene that stably interacts with the plasma membrane and regulates activation of selective signaling pathways via lateral diffusion and interaction with other molecules (48–50). Thus, several lines of investigation might be pursued to determine mechanism by which anti-EMP2 diabodies elicit apoptosis.

In conclusion, treatment of endometrial adenocarcinoma cells with our highly specific anti-EMP2 diabody resulted in a significant increase in caspase-dependent apoptotic cell death in vitro and a reduction in tumor volume in vivo. These data support our previous finding that EMP2 positively correlates with the tumor phenotype of EC. Together, these results suggest that EMP2 may serve as a therapeutic target. Additional experiments will be necessary to determine the preclinical utility of EMP2 diabodies for EC treatment.

Acknowledgments

Financial Support: NIH HD48540 (JB), CA86306 (AMW, JB), CA009120 (MW), 2-T32-AI-07323 (KS) and CA016042 (UCLA Jonsson Comprehensive Cancer Center flow cytometry core); Iris Cantor Seed Grant (MW), and the Giannini Family Foundation (MW), U54 CA119367 (MW), and the Oppenheimer Family Foundation Grant-Center for the Prevention of Eye Disease (LKG).

Abbreviations

EMP2	epithelial membrane protein 2
GAS3/PMP22	growth arrest specific gene 3/peripheral myelin protein 22
EC	endometrical cancer
GEM	glycolipids-enriched lipid raft microdomain
scFv	single chain Fv
VH	heavy chain variable region
VL	light chain variable region
7AAD	7-aminoactinomycin D

References

1. American Cancer Society. Cancer Facts and Figures 2006. 2006. Available at http://www.cancer.org/downloads/STT/CAFF2006PWSecured.pdf
2. Hecht JL, Mutter GL. Molecular and pathologic aspects of endometrial carcinogenesis. J Clin Oncol. 2006; 24:4783–91. [PubMed: 17028294]
3. Sherman ME. Theories of endometrial carcinogenesis: a multidisciplinary approach. Mod Pathol. 2000; 13:295–308. [PubMed: 10757340]
4. Creasman WT. Endometrial cancer: incidence, prognostic factors, diagnosis, and treatment. Semin Oncol. 1997; 24:S1-140–S1-50. [PubMed: 9045311]
5. Markman M. Unresolved issues in the chemotherapeutic management of gynecologic malignancies. Semin Oncol. 2006; 33:S33–8. [PubMed: 16716801]
6. Engleman MA, Small W Jr. Combined modality therapy in the treatment of gynecologic malignancies. Semin Oncol. 2003; 30:80–94. [PubMed: 12908139]
7. Kelloff GJ, Lippman SM, Dannenberg AJ, et al. Progress in chemoprevention drug development: the promise of molecular biomarkers for prevention of intraepithelial neoplasia and cancer--a plan to move forward. Clin Cancer Res. 2006; 12:3661–97. [PubMed: 16778094]
8. Gossett DR, Alo P, Bristow RE, et al. Inability of immunohistochemistry to predict clinical outcomes of endometrial cancer patients. IntJ GynecolCancer. 2004; 14:145–51.
9. Wadehra M, Iyer R, Goodglick L, Braun J. The tetraspan protein epithelial membrane protein-2 interacts with beta1 integrins and regulates adhesion. J Biol Chem. 2002; 277:41094–100. [PubMed: 12189152]
10. Wadehra M, Goodglick L, Braun J. The tetraspan protein EMP2 modulates the surface expression of caveolins and glycosylphosphatidyl inositol-linked proteins. Mol Biol Cell. 2004; 15:2073–83. [PubMed: 14978215]
11. Wadehra M, Su H, Gordon LK, Goodglick L, Braun J. The tetraspan protein EMP2 increases surface expression of class I major histocompatibility complex proteins and susceptibility to CTL-mediated cell death. Clin Immunol. 2003; 107:129–36. [PubMed: 12763482]
12. Leitinger B, Hogg N. The involvement of lipid rafts in the regulation of integrin function. J Cell Sci. 2002; 115:963–72. [PubMed: 11870215]
13. Moffett S, Brown DA, Linder ME. Lipid-dependent targeting of G proteins into rafts. J BiolChem. 2000; 275:2191–8.
14. Abrami L, Fivaz M, Kobayashi T, Kinoshita T, Parton RG, van der Goot FG. Cross-talk between caveolae and glycosylphosphatidylinositol-rich domains. J Biol Chem. 2001; 276:30729–36. [PubMed: 11406621]
15. Galbiati F, Razani B, Lisanti MP. Emerging themes in lipid rafts and caveolae. Cell. 2001; 106:403–11. [PubMed: 11525727]
16. Gruenberg J, Maxfield FR. Membrane transport in the endocytic pathway. Curr Opin Cell Biol. 1995; 7:552–63. [PubMed: 7495576]

17. Wadehra M, Forbes A, Pushkarna N, et al. Epithelial membrane protein-2 regulates surface expression of alphavbeta3 integrin in the endometrium. Dev Biol. 2005; 287:336–45. [PubMed: 16216233]
18. Morales S, Mareninov S, Wadehra M, Braun J, Gordon LK. FAK-Src Regulated PVR Response is EMP2 Dependent. 2008 Submitted.
19. Wadehra M, Dayal M, Mainigi M, et al. Knockdown of the tetraspan protein epithelial membrane protein-2 inhibits implantation in the mouse. Dev Biol. 2006; 292:430–41. [PubMed: 16487956]
20. Wadehra M, Forbes A, Pushkarna N, et al. Epithelial membrane protein-2 regulates surface expression of alphavbeta3 integrin in the endometrium. Dev Biol. 2005; 287:336–45. [PubMed: 16216233]
21. Wadehra M, Natarajan S, Seligson DB, et al. Expression of epithelial membrane protein-2 is associated with endometrial adenocarcinoma of unfavorable outcome. Cancer. 2006; 107:90–8. [PubMed: 16736513]
22. Marks JD, Bradbury A. Selection of human antibodies from phage display libraries. Methods Mol Biol. 2004; 248:161–76. [PubMed: 14970495]
23. Holliger P, Prospero T, Winter G. “Diabodies”: small bivalent and bispecific antibody fragments. Proc Natl Acad Sci U S A. 1993; 90:6444–8. [PubMed: 8341653]
24. Olafsen T, Cheung CW, Yazaki PJ, et al. Covalent disulfide-linked anti-CEA diabody allows site-specific conjugation and radiolabeling for tumor targeting applications. Protein Eng Des Sel. 2004; 17:21–7. [PubMed: 14985534]
25. Blazek D, Celer V, Navratilova I, Skladal P. Generation and characterization of single-chain antibody fragments specific against transmembrane envelope glycoprotein gp46 of maedi-visna virus. J Virol Methods. 2004; 115:83–92. [PubMed: 14656464]
26. Wang CX, Wadehra M, Fisk BC, Goodglick L, Braun J. Epithelial membrane protein 2, a 4-transmembrane protein that suppresses B-cell lymphoma tumorigenicity. Blood. 2001; 97:3890–5. [PubMed: 11389031]
27. Gussow D, Clackson T. Direct clone characterization from plaques and colonies by the polymerase chain reaction. Nucleic Acids Res. 1989; 17:4000. [PubMed: 2734114]
28. Marks JD, Hoogenboom HR, Bonnert TP, McCafferty J, Griffiths AD, Winter G. By-passing immunization. Human antibodies from V-gene libraries displayed on phage. J Mol Biol. 1991; 222:581–97. [PubMed: 1748994]
29. Schier R, Bye J, Apell G, et al. Isolation of high-affinity monomeric human antic-erbB-2 single chain Fv using affinity-driven selection. J Mol Biol. 1996; 255:28–43. [PubMed: 8568873]
30. Adams GP, Schier R, McCall AM, et al. Prolonged in vivo tumour retention of a human diabody targeting the extracellular domain of human HER2/neu. Br J Cancer. 1998; 77:1405–12. [PubMed: 9652755]
31. Wadehra, M.; Mainigi, M.; Morales, S.; Rao, RG.; Gordon, LK.; Braun, J. Steroid Hormone regulation of EMP2 expression and localization in the endometrium. 2007. Submitted
32. Agus DB, Scher HI, Higgins B, et al. Response of Prostate Cancer to Anti-Her-2/neu Antibody in Androgen-dependent and -independent Human Xenograft Models. Cancer Res. 1999; 59:4761–4. [PubMed: 10519379]
33. Cochlovius B, Kipriyanov SM, Stassar MJ, et al. Treatment of human B cell lymphoma xenografts with a CD3 × CD19 diabody and T cells. J Immunol. 2000; 165:888–95. [PubMed: 10878363]
34. Myers SA, Clements JA. Kallikrein 4 (KLK4), a new member of the human kallikrein gene family is up-regulated by estrogen and progesterone in the human endometrial cancer cell line, KLE. J Clin Endocrinol Metab. 2001; 86:2323–6. [PubMed: 11344246]
35. Schneider CC, Gibb RK, Taylor DD, Wan T, Gercel-Taylor C. Inhibition of endometrial cancer cell lines by mifepristone (RU 486). J Soc Gynecol Investig. 1998; 5:334–8.
36. Wu AM, Senter PD. Arming antibodies: prospects and challenges for immunoconjugates. NatBiotechnol. 2005; 23:1137–46.
37. Adams GP, McCartney JE, Tai MS, et al. Highly specific in vivo tumor targeting by monovalent and divalent forms of 741F8 anti-c-erbB-2 single-chain Fv. Cancer Res. 1993; 53:4026–34. [PubMed: 7689421]

38. Colcher D, Pavlinkova G, Beresford G, Booth BJ, Choudhury A, Batra SK. Pharmacokinetics and biodistribution of genetically-engineered antibodies. Q J Nucl Med. 1998; 42:225–41. [PubMed: 9973838]
39. Milenic DE, Yokota T, Filpula DR, et al. Construction, binding properties, metabolism, and tumor targeting of a single-chain Fv derived from the pancarcinoma monoclonal antibody CC49. Cancer Res. 1991; 51:6363–71. [PubMed: 1933899]
40. Yokota T, Milenic DE, Whitlow M, Schlom J. Rapid tumor penetration of a single-chain Fv and comparison with other immunoglobulin forms. Cancer Res. 1992; 52:3402–8. [PubMed: 1596900]
41. Holliger P, Hudson PJ. Engineered antibody fragments and the rise of single domains. Nat Biotechnol. 2005; 23:1126–36. [PubMed: 16151406]
42. Nielsen UB, Adams GP, Weiner LM, Marks JD. Targeting of bivalent anti-ErbB2 diabody antibody fragments to tumor cells is independent of the intrinsic antibody affinity. Cancer Res. 2000; 60:6434–40. [PubMed: 11103810]
43. Shimazaki K, Wadehra M, Forbes A, et al. Epithelial membrane protein 2 modulates infectivity of Chlamydia muridarum (MoPn). Microbes Infect. 2007; 9:1003–10. [PubMed: 17544801]
44. Mould AP, Humphries MJ. Regulation of integrin function through conformational complexity: not simply a knee-jerk reaction? CurrOpinCell Biol. 2004; 16:544–51.
45. Renshaw MW, Price LS, Schwartz MA. Focal adhesion kinase mediates the integrin signaling requirement for growth factor activation of MAP kinase. J Cell Biol. 1999; 147:611–8. [PubMed: 10545504]
46. Zhao JH, Reiske H, Guan JL. Regulation of the cell cycle by focal adhesion kinase. J Cell Biol. 1998; 143:1997–2008. [PubMed: 9864370]
47. Rupinder SK, Gurpreet AK, Manjeet S. Cell suicide and caspases. Vascul Pharmacol. 2007; 46:383–93. [PubMed: 17382599]
48. Enomoto T, Fujita M, Inoue M, Tanizawa O, Nomura T, Shroyer KR. Analysis of clonality by amplification of short tandem repeats. Carcinomas of the female reproductive tract. Diagn Mol Pathol. 1994; 3:292–7. [PubMed: 7866641]
49. Enomoto T, Fujita M, Inoue M, et al. Alterations of the p53 tumor suppressor gene and its association with activation of the c-K-ras-2 protooncogene in premalignant and malignant lesions of the human uterine endometrium. Cancer Res. 1993; 53:1883–8. [PubMed: 8385572]
50. Niv H, Gutman O, Kloog Y, Henis YI. Activated K-Ras and H-Ras display different interactions with saturable nonraft sites at the surface of live cells. J Cell Biol. 2002; 157:865–72. [PubMed: 12021258]

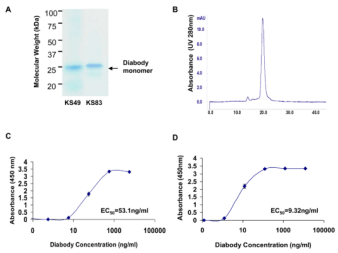

Figure 1. Biochemical characterization of constructed diabodies

(A) SDS-PAGE and Coomassie staining analysis of purified diabodies. Lane 1: KS49; Lane 2: KS83. Arrow indicates an appropriate molecular weight of diabody monomer. (B) Size-exclusion FPLC of purified diabody on a Superdex 75 column. Retention time of each sample was compared with appropriate molecular weight standards. (C) ELISA dose-response assay of KS49 diabody. Plates were coated with hEMP2 peptides, and 10-fold delusions (1:10-1:1×10^5) of the diabody preparations were assayed for binding. (D) ELISA dose-response assay of KS83 diabody. Plates were coated with mEMP2 peptides, and 10-fold delusions (1:10 to 1:1 × 10^6) of the diabody preparations were assayed for binding. For (C) and (D), EC_{50} was calculated. Results are representative of 3 independent experiments.

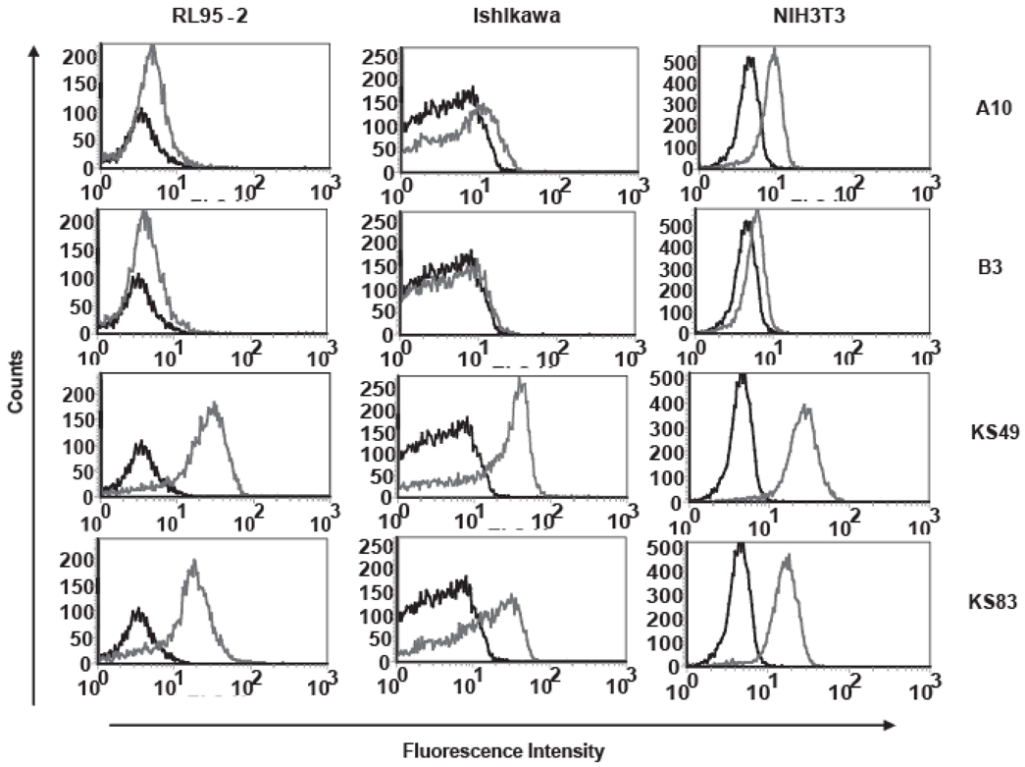

Figure 2. Cellular binding analysis of purified diabodies using flow cytometry

Cellular binding of purified diabodies (labeled on right) was tested on RL95-2, Ishikawa, and NIH 3T3 cells using flow cytometry. Three independent experiments were performed with similar results; a representative graph is shown.

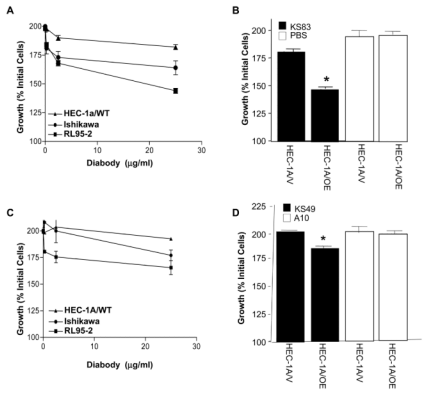

Figure 3. Diabodies induce cytostasis

0-to-25 μg/ml of diabody KS83 (A) or KS49 (B) were added to endometrial carcinoma cell lines HEC-1A, Ishikawa, and RL95-2 in triplicate for 24 hours. Cytostasis was calculated as the ratio of final/initial cells plated using the absorbances at 595nm. (C) 25 μg/ml of diabody KS83 or a vehicle control was added to HEC-1A vector control cells (HEC-1A/V) or cells that overexpress EMP2 (HEC-1A/OE) in triplicate for 24 hours. (D) KS49 or the control diabody A10 was added to HEC-1A/V or HEC-1A/OE cells in triplicate for 24 hours. Comparison by student's t test, * $p<0.05$.

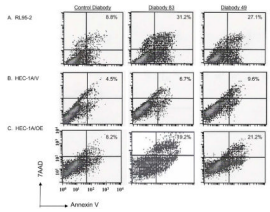

Figure 4. Diabodies promote apoptosis

(A) RL95-2, (B) HEC-1A/V, and (C) HEC-1A/OE cells were incubated with 12.5 μg/ml KS49, KS89, or A10 (control) diabody for 24 hours. Cells were washed and stained with annexin V and 7AAD. Staining is expressed as the % annexin V-7AAD positive cells above the isotype control. The experiment was repeated 3 times with similar results; a representative graph is depicted.

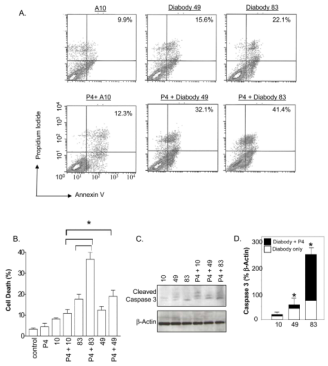

Figure 5. Progesterone augments diabody mediated apoptosis

(A) RL95-2 cells were treated with progesterone P4 (25 μM) or vehicle control (ethanol) in combination with 12.5 μg/ml KS49, KS89, or A10 (control) diabody for 24 hours. Cells were stained for annexin V and propidium iodide, and apoptosis and cell death were further quantitated using flow cytometry. Staining is expressed as the % annexin V-propidium iodide positive cells above the isotope control. (B) RL95-2 cells were treated with progesterone P4 (25 μM) or vehicle control (ethanol) and diabodies KS83, KS49, or A10 for 72 hours. Cell death was determined by trypan blue exclusion, and depicted as a % of the total number of cells counted. *$p<0.05$ (C) Apoptosis and cell death were further quantitated using western blot analysis. Cleaved caspase 3 (Δcaspase 3) was assessed after 24 hours of treatment. β-actin serves as the loading control. The experiment was repeated 3 times, and a representative graph is depicted. (D) Statistical analysis of cleaved caspase 3 relative to β-actin expression, compared by student's t test; *$p<0.05$.

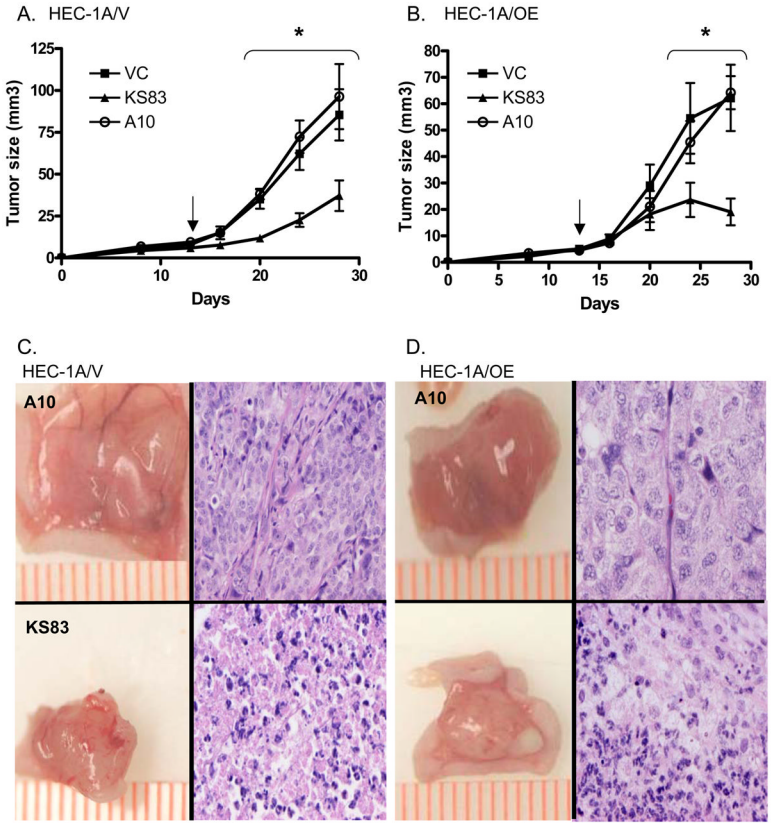

Figure 6. Anti-EMP2 diabodies reduce tumor load in vivo

(A) HEC-1A/V or (B) HEC-1A/OE cells were injected s.c. into nude Balb/c female mice. At day 13 (arrow), mice were injected twice a week with 1 mg/kg of anti-EMP2 diabody 83, control diabody A10, or sterile saline. Tumor volume was calculated using calipers. n=6. At day 31, mice were euthanized and tumor histology was assessed by hemotoxylin and eosin staining. A representative panel depicts excised tumors (left; scalebar, mm) and the corresponding histology (right; 40X magnification) for HEC-1A/V (C) and HEC-1A/OE (D). Comparison by student's t test, *$p<0.05$

Table 1

Effect of parenteral diabody

Mice were injected i.v. with sterile saline, control diabody A10, or anti-EMP2 diabodies (K83 or K49) biweekly for 14 days. 3 mice were utilized per group. Mouse weights were determined at the starting and final day, and serum analytes were determined from blood obtained on the final day.

	Starting Weight	Final Weight	Direct Bilirubin (mg/dL)	Total Bilirubin (mg/dL)	ALT (U/L)
Vehicle Control	19.9 ± 0.7	19.8 ± 0.4	0	0.2	45 ± 6
A10	18.7 ± 0.2	19.5 ± 1.7	0	0.2	36 ± 8
K83	18.9 ± 0.9	19.8 ± 0.9	0	0.2	44 ± 8
K49	19.9 ± 1.4	20.3 ± 0.1	0	0.2	37 ± 7